VIII ECCOMAS Thematic Conference on Smart Structures and Materials
SMART 2017
A. Güemes, A. Benjeddou , J. Rodellar and Jinsong Leng (Eds)

SMART BEHAVIOUR OF CNT MODIFIED ADHESIVE FILMS FOR CARBON FIBER COMPOSITE REPAIR

A. UREÑA, C. GARCÍA-NIETO, X.F. SÁNCHEZ-ROMATE, J. RAMS, M. SÁNCHEZ

Materials Science and Engineering Area
Universidad Rey Juan Carlos (URJC)
Calle Tulipán, s/n, 28933 Móstoles, Madrid, Spain
e-mail: alejandro.urena@urjc.es, www.urjc.es

Key words: Adhesive, repair, composite, SHM, CNT

Abstract. Epoxy adhesives films were doped by spraying an aqueous dispersion of carbon nanotubes. Sensing capability of carbon fiber reinforced composite coupons with bonded patch repairs was evaluated; several single lap shear and Mode-I fracture energy tests were conducted and their electrical responses were characterized. It was observed that electrical resistance increases with mechanical strain due to tunnelling effect on CNT percolating networks and increases of electrical resistance associated to crack propagations could be also detected.

Once the smart behaviour if the adhesive joints was identified by means of mechanical tests in normalized adhesive joined specimens, panels (400 x 400mm) with square co-bonded patches, made using the same curing cycle based on the repaired material one, were prepared using CNT doped adhesive films. These panels were mechanical tested to determine the effect of the doping treatment on the mechanical behaviour of the repairs, at the same time that electric measurements were carried out to identified local failures during testing. Obtained results showed that structural film adhesives could be surface doped with CNT providing sensing capabilities to be used in structural health monitoring of adhesive repairs in composite structures.

1 INTRODUCTION

Composite primary structures repairing is a priority issue in the aerospace industry. When a composite structure suffers an in-service damage, if it is weakened due to fibers breakage or delaminations, it is necessary to make a structural repairing. This kind of repairs, unlike cosmetic or temporary ones, consist on a substitution of damaged fibers and plies in order to restore the original mechanical performance. One of the possible solutions is to apply composite patches by using adhesives [1-2]. However, in order to ensure the quality of these repairs, it is necessary to develop novel inspection techniques, especially non-destructive tests (NDT), such as ultrasounds (C-Scan), vibrothermography or shearograpgy. They are able to detect damage onset in this type of repairs in composite structures [3-4].

An alternative to NDT is providing to the adhesive joint a multifunctional behaviour. The present work aims to analyze the monitoring capability of bonded joints by using adhesive films previously doped with carbon nanotubes (CNT). In previous works, it has been proved that CNT networks are able to properly detect strain and discontinuities (failures) by means of electrical resistance change measurements [5-6].

There are many research in which this CNT network was created by dispersing CNT on a paste adhesive (generally an epoxy based one) using the conventional dispersing techniques (such as three roll mill calendering or toroidal stirring). However, in this work, CNTs were applied directly over the adhesive surface by spraying an aqueous CNT solution [7]. Previously to sensing characterization, a study of the mechanical properties on standardized Mode-I and Single Lap Shear (SLS) specimens has been carried out. Once the multifunctional behaviour of these joints was identified, panels with a composite repair patch were manufactured, using the proposed adhesive. Mechanical testing of these panels has showed the Structural Health Monitoring (SHM) capabilities of CNT doped adhesive joints.

2. EXPERIMENTAL PROCEDURE

2.1 Materials

Adhesive was a FM300, supplied by Cytec. It is an epoxy based adhesive film with a wide-open knit tricot carrier. For the present study, the FM300K was used, with a surface weight of 244 g/m^2, nominal thickness of 0.2 mm, being considered the one with the highest performance within FM300 series. More specifically, it has a shear strength allowable of 36.8 MPa at 24 ºC and 20.4 MPa at 150 ºC.

CNT doping was carried out by spraying an aqueous CNT dispersion over the adhesive surface, using an airbrush. Pressure was set to 0.1 MPa at 40 cm distance. Multiwall CNTs were supplied by Nanocyl, with the commercial name of NC3152, with an average diameter of 9.5 nm and a length up to 1 μm. They have a 90 % C purity and are amino-functionalized. To stabilize the CNT dispersion, a surfactant called sodium dodecyl sulphate (SDS) was used at 1.0 wt. % content. 0.1 wt. % CNT dispersion was achieved by means of ultrasonication, using a horn sonicator of 400 W power and 24 Hz frequency. Sonication was done during 20 min at an irradiation acoustic time of 0.5 s and horn amplitude of 80 %. After sonication process, a centrifugation stage was done at 5000 rpm during 10 min.

CFRP substrates were manufactured by intermediated modulus unidirectional tape prepegs (IMA/M21E). Carbon fiber and prepeg surface weight are 194 ± 5 g/m^2 and 294 ± 9 g/m^2. Resin weight fraction is 34 % and laminate density is 1.58 g/cm^3. Several 500 x 500 mm panels were manufactured at a $[0]_n$ layer sequence with different thickness depending on tests requirements in order to manufacture the normalized coupons for Mode-I and SLS tests. Curing was done in autoclave with a vacuum bag using a double ramp temperature curing cycle. Maximum curing temperature and pressure were 180 ºC and 0.9 MPa respectively, during 8 h.

2.2 Mechanical tests

SLS joints were tested using the AITM 1-0019 standard. Adhesive joints were manufactured by co-bonding. Total thickness of each substrate was 2.024 mm, corresponding to a $[0]_{11}$ layer sequence. Mechanical testing was done at room temperature at a test rate of 0.5 mm/min.

Electrical monitoring of SLS specimens was carried out as shown in Figure 1a. Two electrodes made of copper wire with silver ink were attached to the center of the overlapping area, at 7.5 mm and 12.5 mm distance from the edge in the main load and the transversal direction, respectively. Monitoring was carried out, thus, in the transversal direction of the adhesive joints. Electrical acquisition was carried out by using a digital multimeter Agilent 34410A.

Moreover, Mode-I energy fracture (GIC) tests were conducted in order to determine the strength of the adhesive joints as a function of crack length. These tests were carried out according to AITM 1-0053 standard. The electrical response of the adhesive joints were measure during the mechanical testing. In this case, the total thickness of each substrate was 1.472 mm, corresponding to a $[0]_8$ layer sequence.

Electrical monitoring of Mode-I specimens was done as shown in Figure 1b. Two electrodes made of copper wire with silver ink were attached at 60 mm distance of the load application point. Thus, monitoring was carried out in the transversal direction, like in the SLS specimens.

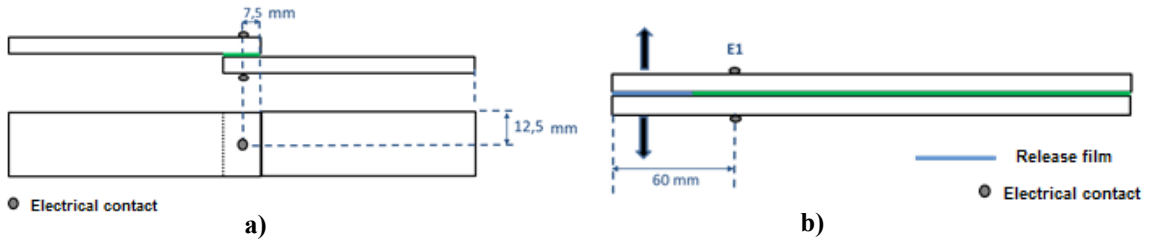

Figure 1: Configurations of electrical contact for sensorization during: a) SLS test; and b) GIC test.

2.3 Panel repair tests

A 400 x 400 mm composite panel was defined with an applied repair. This repair was a composite patch scarf (repair path with a constant slope). The material of the pristine panel was the same as used previously, IMA/M21E. Layer sequence was $(45/-45/90/0/90/-45/45/90/0/90/-45/45/90/0/45/-45)_s$ with a total thickness of 5.888 mm.

The patch repair was manufactured by using the same prepeg. This repair was done over 16 plies with a total thickness of 2.944 mm, being the ply of the base of the cone repair oriented at -45º. The rest of the plies were oriented following a similar stacking sequence than the original laminate. An outer 45º ply was placed over the entire repair. Figure 2 shows a schematic of the

patch repair. Adhesive film was the FM300K with the same cure cycle than previously described.

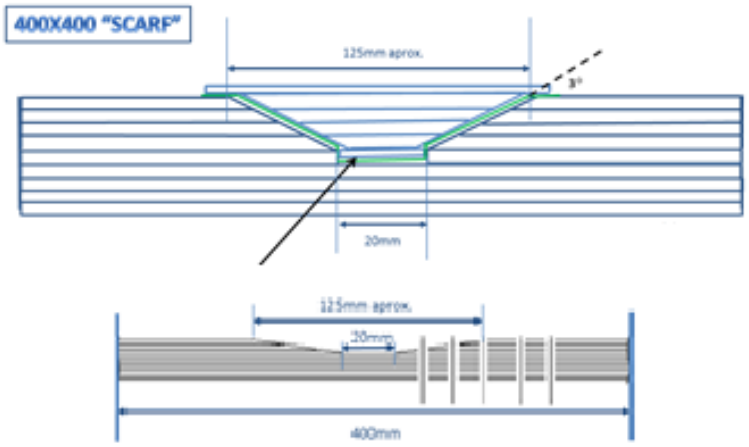

Figure 2: Schematics of the patch repair in a 400 x 400 mm composite panel

Once manufactured, the panel was subjected to mechanical testing in order to prove sensing capabilities of CNT doped adhesive film. The aim was to compare the electrical response of the adhesive with the measurements obtained with conventional strain gauges. This would allow comparing the different technologies (strain gauges, electrical sensing and acoustics), giving a more detailed understanding of the mechanical performance of the panel.

A shear test was carried out in the panel. Six rectangular rosettes RY81-6-350 with 350 Ω and eight strain gauges LY41-6-350 with linear geometry and 350 Ω were placed in the panel. The disposition is shown in Figure 4, where the outer and the inner (Side A and B, respectively) surface of the panel is represented. The outer corresponds to the composite patch repair side. In addition, the corners were cut according to the required tooling for the mechanical tests.

In combination with rosettes and strain gauges, an electrical sensing scheme was defined. This electrical network (blue circles) was composed by five channels (E1 to E5) and it is shown in Figure 3. E1 and E3 were placed in the load axis at 10 mm from the corner of the patch. E2 was placed at 20 mm from the center of the repair. E4 and E5 channels were placed near the right and left corners of the patch at 10 mm.

Figure 4 shows an image of the mechanical test in a tensile testing machine with a 500 kN load cell at a test rate of 0.5 mm/min. Test would end by collapsing of composite panel or by reaching the maximum allowable of the testing machine.

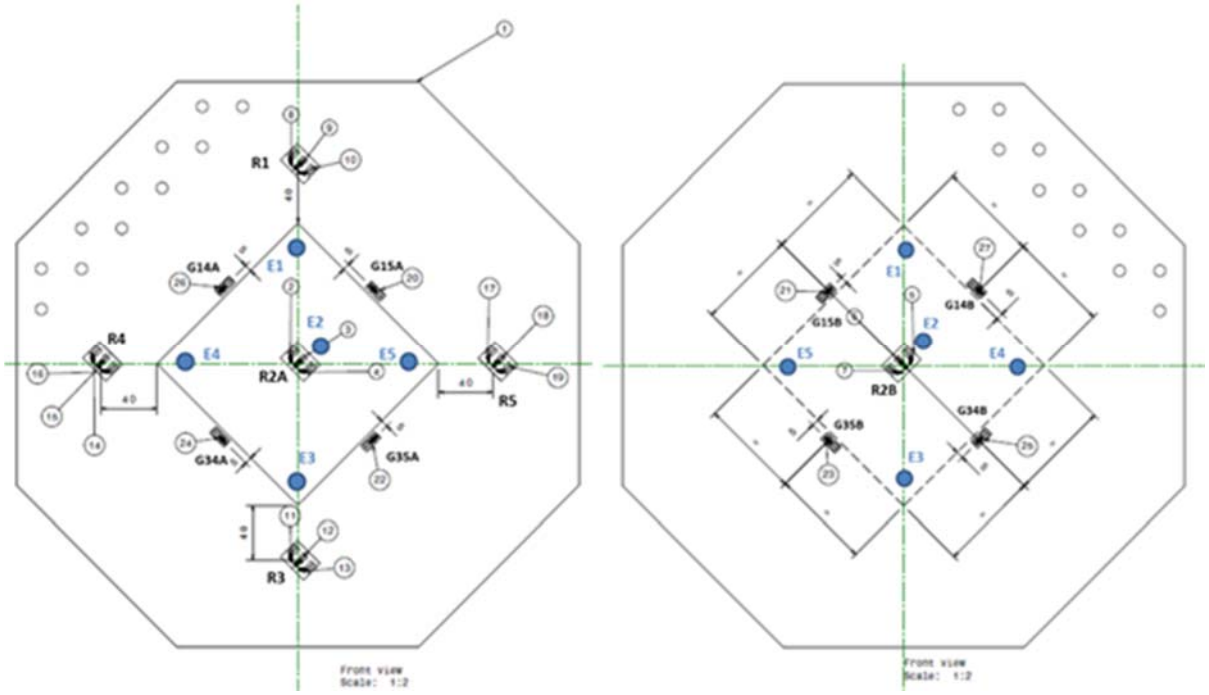

a) b)

Figure 3. Schemes of the extensometry and electric sensorization of a repaired composite panel: a) front face; b) back face.

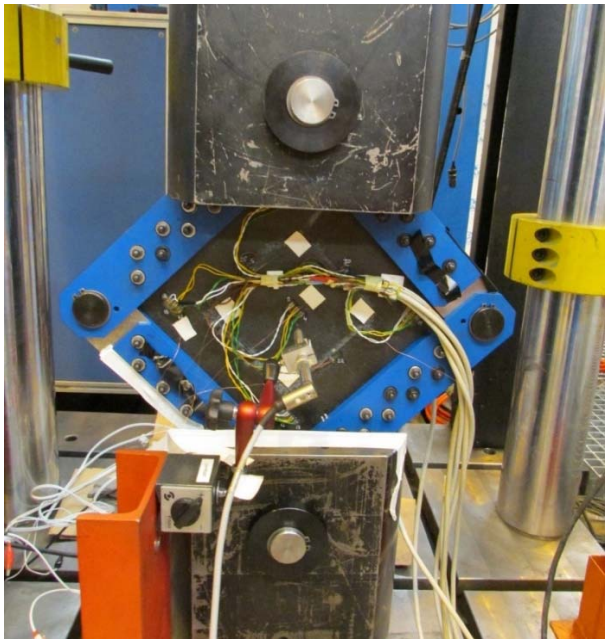

Figure 4. Experimental arrangement of the shear test of the repaired composite panel

2.4 Non-destructive testing

Previously to mechanical testing, composite repaired panel was inspected by ultrasounds. The results did not show neither discontinuities higher than 36 mm^2 nor volumetric porosity. Therefore, from the inspection point of view, the repair was considered valid. After mechanical testing, ultrasonic inspection was carried out again and the discontinuities and defects were characterized, allowing correlating the electrical response with the NDT results.

3 RESULTS AND DISCUSSION

The electrical monitoring of SLS joints could lead to different behaviours on the electrical response, defined as Type I and II, which are shown in Figure 5. Both of them presents an initial constant trend, associated to a minimum strain threshold from which the system is able to detect electrical changes. After that, an increase of the electrical resistance is observed, corresponding to higher strain levels. This tendency could be linear or exponential depending on the prevalence of contact and tunnelling effect between adjacent CNTs, respectively. Instabilities may be due to crack initiation as well as local failures (i.e. microcavities, local disbonds). Finally, a sudden increase of the electrical resistance is observed, corresponding to the final failure of the joint.

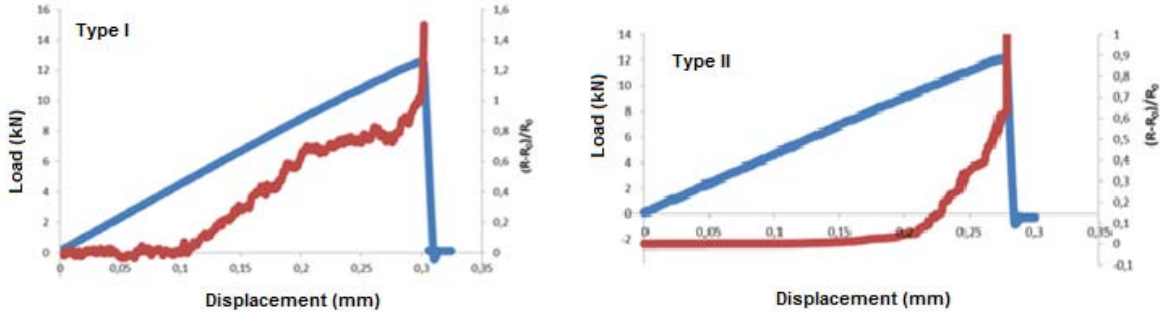

Figure 5. Single lap shear test curves. Mechanical response (blue curve). Electrical response (red curve).

On the other hand, electromechanical curves of Mode-I test specimens allow correlating the electrical response of the joint with the crack propagation. Figure 6 shows an example of these curves. An initial stage with a slight increase of the electrical resistance is observed just before crack initiation and due to adhesive deformation. When crack initiation took place, a sharp rise of the electrical resistance is noticed due to breakage of conductive pathways. From this point, a steady increase of the electrical resistance as well as sudden rises are observed. This is due to the combination of two effects, the adhesive deformation and the breakage of electrical pathways along the joint. Sudden drops can be also associated to the presence of microcavities as commented before on SLS tests. The test was ended once crack length was 60 mm from the initial pre-crack, correlated to a piano hinge displacement of 26 mm. For that reasons, a sudden change of the electrical resistance is not observed at the end of the test because Mode-I specimen was not totally broken.

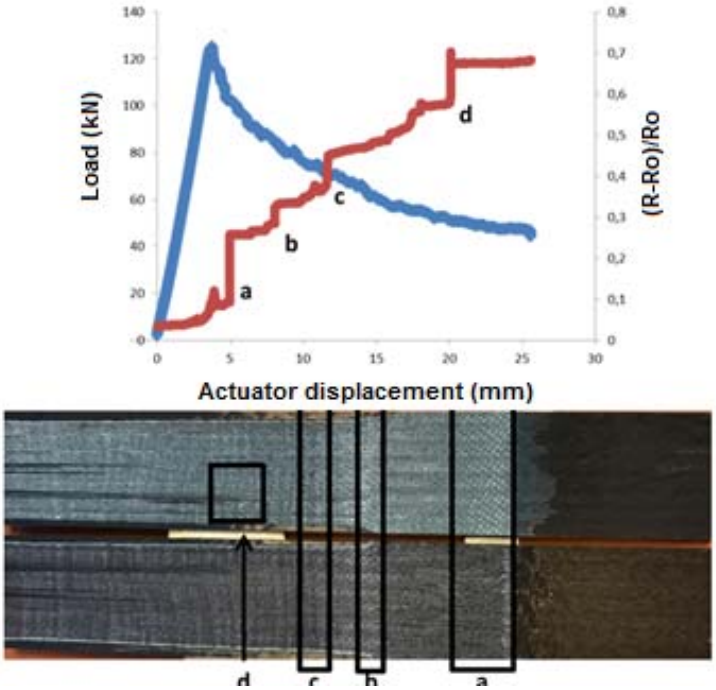

Figure 6. GIC test curves. Mechanical response (blue curve). Electrical response (red curve). Correlation with failure mode.

The analysis of the fractured surfaces of Mode-I specimens, once they were totally open, shows a clear correlation between changes on failure modes and the sudden changes observed in the electrical resistance during crack propagation. Although the mechanical curve does not present the typical behaviour of an unstable crack growing (called *stick-slip* behaviour), the fractured surface and the electrical response clearly show this unstable behaviour. Figure 6 correlates the sudden changes of the electrical resistance (a, b, c and d points) with the different failure modes. Thus, at points a and c, a change from type D, that is, interface failure between the uncured substrate and the adhesive film, to type E failure, that is, interface failure between the cured substrate and the adhesive film, is observed whereas at points b and d the change in the failure mode is the opposite.

Regarding to the repaired panel, the NDT inspection after the test showed the presence of two disbond areas (Figure 7):

- **Disbond area *A*:** it was detected in the upper region of the patch repair. It was not possible to determine if the bottom echo came from the interface between the substrate and the adhesive film (adhesive failure) or inside the adhesive (cohesive failure). Damage extent was similar to an equilateral triangle of 10 mm.

- **Disbond area *B*:** it was detected in the lower region of the patch repair with dimensions of 61 x 10 mm^2, approximately. Similarly to disbond area *A*, it was not possible to determine if the failure was located in the interface between substrate and adhesive film or inside the adhesive

Figure 7. Ultrasonic inspection of repaired panel after shear testing.

The results obtained by the sound level meter during the mechanical test are shown in Figure 8. The environmental sound was between 69 and 71 dB. By taking into account this reference, several sounds at different magnitude were detected. The first one of them was detected at 283 kN with a magnitude of 79 dB. Then, the second one was detected at 297 kN, reaching a value of 80 dB. After 330 kN, several sounds were recorded with higher intensities: at 332 kN, a sound with a magnitude of 87 dB was detected; at 337 kN, the acoustic emission reached a value of 90 dB; and at 344 kN, the highest acoustic emission was detected, with a value of 111 dB. From this point until the end of the test (430 kN), no more anomalous sounds were recorded.

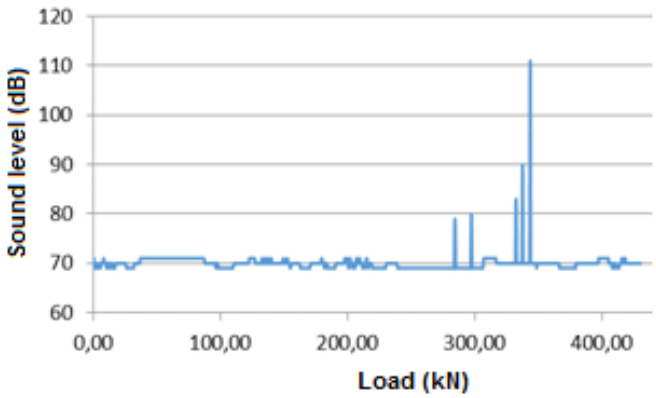

Figure 8. Detected sounds during mechanical testing of repaired panel

Finally, a correlation between inspection, acoustic emission and strain gauges and electrical sensing was established. The results of sensing and strain gauges for loads of 332 kN and 367 kN do not show variations that could be correlated to disbonds.

The analysis at 337 kN showed that the most significant variation on the strain gauge and sensing curves took place at the E1 channel. Figure 9 shows the electrical response of the E1 channel and the strain gauge response of the nearest rosette, R1 from 0 to 430 kN. At 337 kN, a sudden change on the electrical curve, R1_c was observed. In addition, a disbond were also observed in the area *A*. Therefore, it can be concluded that the disbond took place at 337 kN.

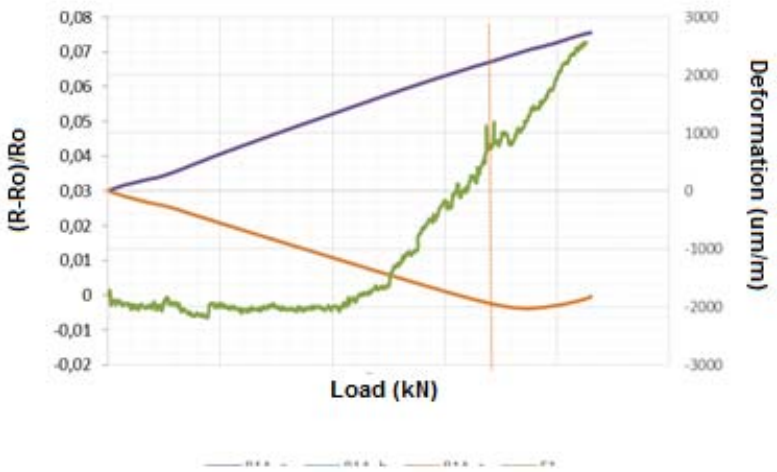

Figure 9. Correlation between extensometric measurements and electrical sensorization for emitted sound at 337 kN

On the other hand, the most significant changes on the sensing and strain gauge curve at 344 kN took place in the E3 and E5 channels. Figure 10 shows the strain gauge response of the nearest rosettes, G35A and G35B in combination with the electrical response. At 344 kN, a noticeable change on G35A and G35B curves was observed. As a disbond was detected during the inspection phase, it can be concluded that it took place at 344 kN.

A complete analysis of electromechanical curves of E1 and E3 channels allows to distinguish two regions:

a) The region (I) under 220 kN in which the normalized resistance presents a slight decrease up to minimum values of 0.25 and 1 %, respectively. This decrease of the electrical resistance has been already explained in previous studies [8-9], being associated to local compressions through thickness during the test leading to the formation of new electrical pathways. By taking into account the panel geometry in the upper region of the patch repair, the compression effect takes place in the initial stage of the mechanical test, until a strain threshold is reached.

b) The second region (II) takes place from 220 kN until the end of the test. It is characterized by a progressive increase of the electrical resistance with strain. The results are similar to those observed for the normalized SLS coupons. As commented before, higher deformations leads to lower conductivities as the distance between adjacent particles is increased.

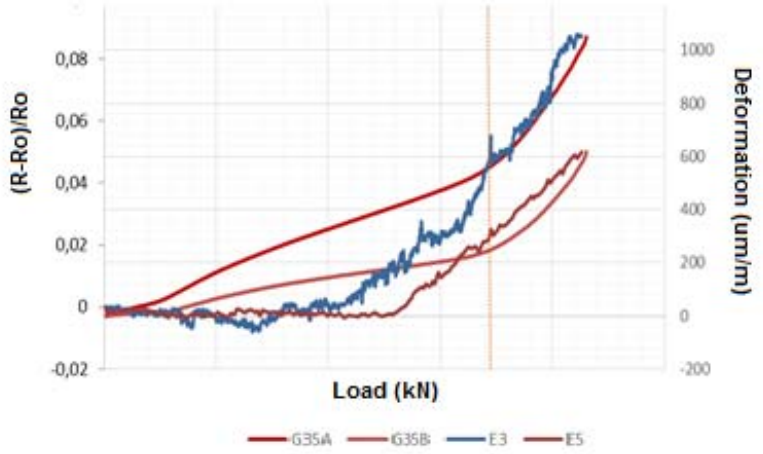

Figure 10. Correlation between extensometric measurements and electrical sensorization for emitted sound at 344 kN

Moreover, the detected disturbances on E1 and E3 channels could be explained by assuming that, once disbond takes place suddenly, the contact surfaces can be touching again. This would explain the rises and drops of the electrical resistance.

4. CONCLUSIONS

- Surface doped adhesive films with 0.1 wt. % CNT are able to evaluate the mechanical integrity of CFRP co-bonded joints.
- SLS tests prove the potential of the proposed adhesives to monitor properly the deformation with applied force. Moreover, the final failure is clearly detected by electrical sensing.
- Mode-I tests prove the ability of CNT doped adhesive to monitor crack propagation. It allows to distinguish between different failure modes and mechanical behaviors.
- A composite structural repair done with this adhesive film can be monitored during deformation. The sensitivity of CNT networks allows to detect disbonds that are efficiently detected with other inspection techniques

ACKNOWLEDGEMENTS

The author would like to acknowledge the *Comunidad de Madrid Government* [Program MULTIMAT-CHALLENGE S2013/MIT-2862] and the *Ministerio de Economía y Competitividad* of the Spanish Government [Project MAT2016-78825-C2-1-R] for their financial support.

REFERENCES

[1] K.B. Katnam a,n, L.F.M.DaSilva b, T.M.Young. "Bonded repair of composite aircraft structures: A review of scientific challenges and opportunities." Composites Part A: Applied Science and Manufacturing. 43, 1587-1598, 2012.

[2] C.H. Wang, A.J. Gunnion. ".Optimum shapes of scarf repairs". Composites Part A: Applied Science and Manufacturing. 40, 1407–1418, 2009.

[3] L. Pieczonka, W.J. Staszewski, T. Uhl, S. Pavlopoulou, C. Soutis. "Nondestructive testing of composite patch repairs". 11th European Conference on Non-Destructive Testing (ECNDT 2014), October 6-10, 2014, Prague, Czech Republic.

[4] M. Genest M. Martinez, N. Mrad G. Renaud,A. Fahr: Pulsed thermography for non-destructive evaluation and damage growth monitoring of bonded repairs. Composite Structures. 88, 112–120, 2009.

[5] J. Rams J, M. Sánchez A. Ureña, A Jiménez-Suárez, M. Campo A Güemes. "Use of carbon nanotubes for strain and damage sensing of epoxy-based composites". International Journal of Smart and Nano Materials, 3, 152–161 (2012)

[6] R. Moriche, M Sánchez, S.G. Prolongo, A. Jiménez-Suárez, A. Ureña. "Structural health monitoring in multiscale composite materials: Nanoreinforced epoxy matrices and coated fabrics". 8th European Workshop on Structural Health Monitoring, EWSHM 2016, vol. 3 (2016).

[7] A. Ureña, M. Sánchez, J. Rams, C. García-Nieto. "Adhesivo tipo film, dispositivo y método para evaluar la integridad estructural de uniones pegadas". Patent N. ES2574443. Expedition date: 10/03/2017.

[8] D. Zhang, L. Ye, D. Wang, Y. Tang, S. Mustapha, Y. Chen. "Assessment of transverse impact damage in GF/EP laminates of conductive nanoparticles using electrical resistivity tomography." Composites Part A: Applied Science and Manufacturing, vol. 43, 1587-1598, 2012.

[9] R. Moriche. "Desarrollo de sensores estructurales de resinas epoxi basados en nanopartículas de grafeno." Doctoral Thesis. Universidad Rey Juan Carlos, 2015.